Mon. Not. R. Astron. Soc. **398,** 715–721 (2009) doi:10.1111/j.1365-2966.2009.15195.x

The escape of ionizing photons from supernova-dominated primordial galaxies

Hidenobu Yajima,[1★] Masayuki Umemura,[1★] Masao Mori[1★] and Taishi Nakamoto[2★]

[1]*Center for Computational Sciences, University of Tsukuba, Tsukuba 305-8577, Japan*
[2]*Earth and Planetary Sciences, Tokyo Institute of Technology, 2-12-1 Ookayama, Meguro-ku, Tokyo 152-8551, Japan*

Accepted 2009 June 2. Received 2009 June 2; in original form 2009 February 10

ABSTRACT

In order to assess the contribution of Lyman break galaxies (LBGs) and Lyman α emitters (LAEs) at redshifts $3 < z < 7$ to the ionization of intergalactic medium (IGM), we investigate the escape fractions of ionizing photons from supernova-dominated primordial galaxies by solving the three-dimensional (3D) radiative transfer. The model galaxy is employed from an ultra-high-resolution chemodynamic simulation of a primordial galaxy by Mori & Umemura, which well reproduces the observed properties of LAEs and LBGs. The total mass of model galaxy is 10^{11} M$_{\odot}$. We solve not only photoionization but also collisional ionization by shocks. In addition, according to the chemical enrichment, we incorporate the effect of dust extinction, taking the size distributions of dust into account. As a result, we find that dust extinction reduces the escape fractions by a factor of 1.5–8.5 in the LAE phase and by a factor of 2.5–11 in the LBG phase, while the collisional ionization by shocks increases the escape fractions by a factor of ≈2. The resultant escape fractions are 0.07–0.47 in the LAE phase and 0.06–0.17 in the LBG phase. These results are well concordant with the recent estimations derived from the flux density ratio at 1500 to 900 Å of LAEs and LBGs. Combining the resultant escape fractions with the luminosity functions of LAEs and LBGs, we find that high-z LAEs and LBGs can ionize the IGM at $z = 3$–5. However, ionizing radiation from LAEs as well as LBGs falls short of ionizing the IGM at $z > 6$. That implies that additional ionization sources may be required at $z > 6$.

Key words: radiative transfer – dust, extinction – galaxies: evolution – galaxies: formation – galaxies: high-redshift.

1 INTRODUCTION

One of momentous issues regarding the evolution of intergalactic medium (IGM) is the ionization history of the Universe, which significantly influences the galaxy formation (e.g. Susa & Umemura 2000; Umemura, Nakamoto & Susa 2001; Susa & Umemura 2004). The *Wilkinson Microwave Anisotropy Probe* (*WMAP*) results provide a wealth of information about the cosmic reionization (Page et al. 2007; Dunkley et al. 2009). However, the detailed history of reionization and the nature of ionizing sources are not yet fully understood. Haardt & Madau (1996) pointed out that the UV background radiation is dominated by quasars at $z < 4$. Fan et al. (2001) showed, using the Sloan Digital Sky Survey (SDSS) sample, that the bright-end slope of the quasar luminosity function at $z \gtrsim 4$ is considerably shallower than that at low redshifts, and concluded that quasars cannot maintain the ionization of IGM at $z \gtrsim 4$. Subsequently, there has been a great deal of discussion regarding the possibility that the IGM is ionized mainly by UV radiation from high-z star-forming galaxies like Lyman break galaxies (LBGs) and Lyman α emitters (LAEs) (e.g. Fan et al. 2006; Bouwens et al. 2007; Gnedin 2008). However, the estimate of the contribution of LBGs or LAEs suffers significantly from the ambiguity regarding the escape fractions of ionizing photons from star-forming galaxies (Razoumov & Sommer-Larsen 2006; Gnedin, Kravtsov & Chen 2008).

Observationally, the escape fractions of ionizing photons are assessed by the relative escape fractions $f_{\rm esc,rel}$, using the flux density ratio at 1500 to 900 Å, $(F1500/F900)_{\rm obs}$, which are defined by

$$f_{\rm esc,rel} = \frac{(L1500/L900)_{\rm int}}{(F1500/F900)_{\rm obs}} \exp\left(\tau_{900}^{\rm IGM}\right), \quad (1)$$

where $\tau_{900}^{\rm IGM}$ represents the line-of-sight opacity of the IGM for 900 Å photons. Normally, the intrinsic luminosity density ratio at 1500 to 900 Å, $(L1500/L900)_{\rm int}$, is assumed to be 3 as a fiducial value. Steidel, Pettini & Adelberger (2001) found $f_{\rm esc,rel} \gtrsim 0.5$ from the composite spectrum of 29 LBGs at $z \sim 3$, and Giallongo et al. (2002)

★E-mail: yajima@ccs.tsukuba.ac.jp (HY); umemura@ccs.tsukuba.ac.jp (MU); mmori@ccs.tsukuba.ac.jp (MM); nakamoto@geo.titech.ac.jp (TN)

and Inoue et al. (2005) estimated the upper limit of $f_{\rm esc,rel} \lesssim 0.1$–0.4 for some LBGs at $z \sim 3$. The direct detection of ionizing photons from high-z star-forming galaxies has been accomplished recently as a consequence of intensive and continuous exertion. Shapley et al. (2006) detected the escaping ionizing photons from two LBGs in the SSA22 field at $z = 3.1$ and they estimated the average relative escape fraction $f_{\rm esc,rel} = 0.14$. Moreover, Iwata et al. (2009) successfully detected the Lyman continuum emission from 10 LAEs and seven LBGs within 198 spectroscopically confirmed samples of LAEs and LBGs in the SSA22 field. They have shown that the mean value of relative escape fractions for seven LBGs is 0.11 after a correction for dust extinction and can be 0.20 if IGM extinction is taken into account.

Theoretically, the accurate estimation of escape fractions requires the three-dimensional (3D) radiative transfer calculations of ionizing photons travelling in inhomogeneous interstellar medium (ISM). Such 3D radiative transfer calculations are fairly recent attempts, because a great deal of computation is required. First, Ciardi, Bianchi & Ferrara (2002) calculated the escape fractions in simple model clouds, where the density distributions are smoothed Gaussian or fractal inhomogeneous. More recently, using gasdynamical simulations of galaxy formation, the escape fractions are estimated by solving 3D radiative transfer. Razoumov & Sommer-Larsen (2006, 2007) have found that the escape fractions decline from several per cent at $z = 3.6$ to 0.01–0.02 at $z = 2.39$, due to higher gas clumping at lower redshifts. But, in these simulations, the effects of dust extinction are not taken into account. Gnedin et al. (2008) performed a cosmological simulation on the formation of a disc-like galaxy that provides the 3D distributions of absorbing gas in and around the galaxy. Then, 3D radiative transfer was solved by including the dust extinction. As a result, the escape fractions turned out to be as low as a few per cent. In this model, the bulk of stars are embedded deep inside the optically thick H I disc and therefore most of ionizing photons emitted from hot stars are absorbed by neutral hydrogen in the H I disc. Only a small fraction of ionizing photons from the stars that are located near the edge of disc can escape from the galaxy. Hence, almost regardless of the effects of dust extinction, the resultant escape fractions become quite small. It implies that star-forming galaxies cannot give a significant contribution to the IGM ionization at $z \gtrsim 3$. For higher redshift $z \gtrsim 8$, on the other hand, some numerical simulations have already shown that large escape fractions of some tens of per cent are possible for low-mass galaxies, which include Pop III stars (Kitayama et al. 2004; Whalen, Abel & Norman 2004; Alvarez, Bromm & Shapiro 2006; Wise & Cen 2009). However, in order to assess the contribution of LAEs and LBGs observed at $3 \lesssim z \lesssim 7$ to IGM reionization, we should evaluate the UV escape fractions from more massive galaxies. The escape of UV photons can sensitively depend on the gravitational potential (Kitayama et al. 2004; Whalen et al. 2004). Also, dust extinction should be taken into account in such primordial galaxies.

In this paper, we reconsider the escape fractions of ionizing photons from high-z primordial galaxies by employing a supernova (SN)-dominated primordial galaxy model proposed by Mori & Umemura (2006), which well reproduces the observed properties of LAEs and LBGs. The total mass is $10^{11}\,{\rm M}_{\odot}$, and the star formation with the Salpeter initial mass function (IMF) is included. In this model, stars are distributed more extendedly in the galaxy and the bulk of interstellar gas is collisionally ionized by SN-driven shock. The spread of stellar distributions and the shock heating can lead to diminishing the absorption of ionizing photons and may enhance escape fractions. Here, we perform the 3D radiative transfer calculations including not only the photoheating but also the shock heating. We incorporate the dust extinction that is consistent with the chemical evolution of galaxy. Then, using the resultant escape fractions, we explore whether LAEs and LBGs can contribute to the ionization of IGM in a high-z Universe. In the present analysis, the cosmological parameters are assumed to be $H_0 = 70\,{\rm km\,s^{-1}\,Mpc^{-1}}$, $\Omega_{\rm M} = 0.3$ and $\Omega_{\Lambda} = 0.7$. In Section 2, the model and the numerical method are described. In Section 3, the numerical results on escape fractions are provided. In Section 4, we discuss the contributions of LAEs and LBGs to the IGM ionization. Finally, Section 5 is devoted to the summary.

2 MODEL AND METHOD

As a model galaxy, we adopt the high-resolution hydrodynamic simulations (1024^3 fixed Cartesian grids) by Mori & Umemura (2006), which are coupled with the collisionless dynamics for dark matter particles as well as star particles and also the chemical enrichment. The simulation box size is 134 kpc in physical scales. Mori & Umemura (2006) demonstrated that an early protogalactic evolution with multitudinous Type II supernovae (SNeII) exhibits intense Lyman α emission, well resembling LAEs. Subsequently, the galaxy shifts to a stellar continuum radiation-dominated phase, which appears like LBGs. In the present analysis, the stages from $t_{\rm age} = 0.1$ to 0.3 Gyr are defined to be the LAE phase and the stages from $t_{\rm age} = 0.5$ to 1.0 Gyr are the LBG phase.

As a post-process, we calculate the escape fractions of ionizing photons with an accurate radiation transfer scheme. The data of the hydrodynamic simulations are coarse-grained into 128^3 Cartesian grids to solve radiation transfer. We use the Authentic Radiation Transfer (ART) method developed by Nakamoto, Umemura & Susa (2001). The performance of this scheme has already been reported as part of the comparison study by Iliev et al. (2006a). The radiation transfer equation is solved along 128^2 rays with a uniform angular resolution from each source. At a point of optical depth τ, the specific intensity is given by $I_\nu(\tau) = I_\nu(0)\exp(-\tau)$, where $I_\nu(0)$ is the intrinsic intensity of ionizing radiation and τ is the optical depth of neutral hydrogen and dust. As for scattering photons, we employ the on-the-spot approximation (Osterbrock 1989), in which scattering photons are assumed to be absorbed immediately on the spot. We obtain the ionization structure assuming the ionization equilibrium, $\Gamma^\gamma n_{\rm H\,I} + \Gamma^C n_{\rm H\,I} n_{\rm e} = \alpha_{\rm B} n_{\rm p} n_{\rm e}$, where Γ^γ, Γ^C and $\alpha_{\rm B}$ are the photoionization rate, the collisional ionization rate and the recombination rate to all excited states, respectively. We continue the radiative transfer calculation recurrently until the ionization structure converges. In an SN-dominated model galaxy, the collisional ionization occurs mostly in low-density, high-temperature regions with $n \lesssim 10^{-3}\,{\rm cm^{-3}}$ and $T_{\rm coll} > 10^4$ K. In such regions, stellar UV radiation contributes to the increase of ionization degree, but does not contribute much to the increase of the temperature. On the other hand, neutral regions are photoionized and heated up to $\sim 10^4$ K (Umemura & Ikeuchi 1984; Thoul & Weinberg 1996), when ionizing radiation is irradiated. Hence, in the present analysis, we assume the gas temperature to be $T = \max\{T_{\rm coll}, 10^4\,{\rm K}\}$ in ionized regions, and we do not update the temperature in iteration of radiation transfer calculation. To evaluate the escape fraction of ionizing photons, we count all photons above the Lyman limit that escape from the calculation box.

The number of ionizing photons emitted from source stars is computed based on the theoretical spectral energy distribution (SED) given by a population synthesis scheme, PÉGASE v2.0 (Fioc & Rocca-Volmerange 1997). We assume the Salpeter (1955) initial mass function in the mass range of 0.1–50 $M_\odot$. As for dust grains, we adopt the empirical size distribution $n_d(a_d) \propto a_d^{-3.5}$ (Mathis, Rumpl & Nordsieck 1977) in the range from 0.1 to 1.0 µm, where a_d is the radius of a dust grain. We assume refractory grains like silicates, for which the photodestruction of dust by UV radiation is negligible over the Hubble time-scale (Draine & Salpeter 1979). The dust grains are distributed proportionally to the metallicity calculated in the hydrodynamic simulations with the relation of $m_d = 0.01 m_g(Z/Z_\odot)$, where m_d, m_g and Z are the dust mass, gas mass and metallicity in a grid, respectively. The density in a dust grain is assumed to be 3 g cm^{-3} like silicates. The dust opacity is given by $d\tau_{\rm dust} = Q(\nu)\pi a_d^2 n_d ds$, where $Q(\nu)$, a_d and n_d are the absorption Q-value, dust size and number density of dust grains, respectively. Since the assumed range of dust size is larger than the wavelength of Lyman limit, we assume $Q(\nu) = 1$ for ionizing photons (Draine & Lee 1984).

3 RESULTS

3.1 Galactic evolution

Fig. 1 shows the snapshots for the evolution of model galaxy as a function of redshift from $t_{\rm age} = 0.1$ to 1.0 Gyr. The density of gaseous and stellar components is adopted from Mori & Umemura (2006). The dust density is evaluated by the metallicity. As a result of multiple SN explosions, dust is distributed more extendedly than stars, which is significantly relevant to the absorption of ionizing photons. Bottom panels show the calculated ionization structure in terms of neutral hydrogen fractions $\chi_{\rm H\,I}$.

First, we see the evolution of the model galaxy. At $t_{\rm age} = 0.1$ Gyr, stars form in high-density peaks in sub-galactic condensations and the burst of star formation starts. Then, massive stars in the star-forming regions explode as SNeII one after another. The gas in the

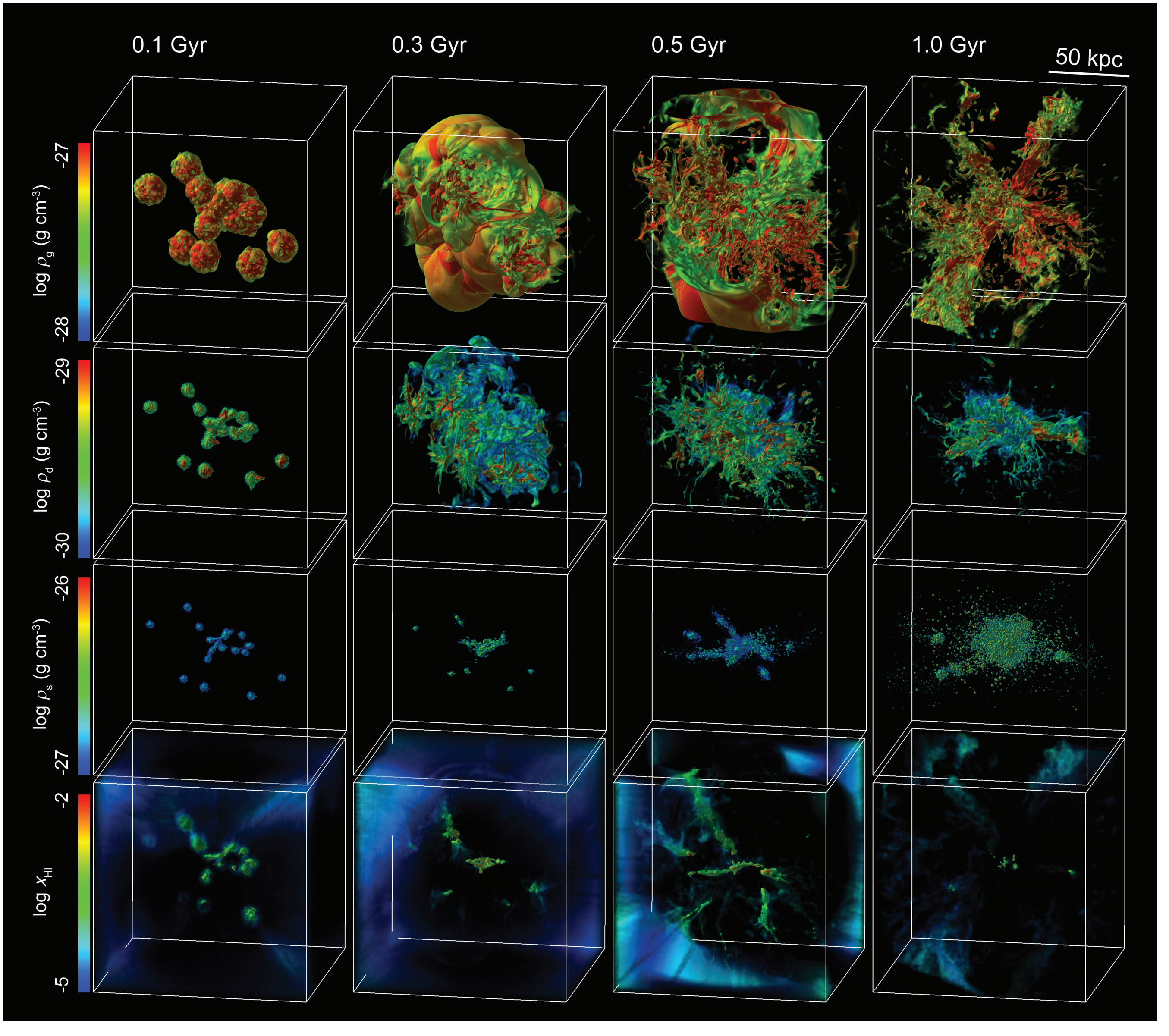

Figure 1. Snapshots of the evolution of the model galaxy with total mass of 10^{11} $M_\odot$ at $t_{\rm age} = 0.1$, 0.3, 0.5 and 1.0 Gyr. Each panel in row corresponds the spatial distributions of gas density ρ_g (g cm^{-3}), dust density ρ_d (g cm^{-3}), stellar density ρ_s (g cm^{-3}) and fractions of neutral hydrogen in logarithmic scale $\chi_{\rm H\,I}$, respectively. The simulation box is 134 kpc in physical scale.

vicinity of SNeII is quickly enriched with the ejected heavy elements and then interstellar dust is locally procreated. However, a large amount of gas still retains a metal- and dust-free state. The spatial distributions of heavy elements are highly inhomogeneous, where gas enriched with $-5.1 \lesssim$ [Si/H] $\lesssim -1.1$ and $-5 \lesssim$ [O/H] $\lesssim -1.0$ coexists with virtually metal-free gas. SN-driven shocks collide with each other to generate large-scale hot ($\gtrsim 10^6$ K) bubbles reaching a higher ionization degree. At $t_{\rm age} = 0.3$ Gyr, roughly 50 per cent of the total volume is highly ionized with $\chi_{\rm H\,I} = 10^{-6}$ to 10^{-7}, where the ionization degree is controlled by the collisional ionization by shock heating and the photoionization by UV radiation from hot young stars. The spatial distributions of the heavy elements are still highly inhomogeneous in the range $-2.5 \lesssim$ [Si/H] $\lesssim -0.5$ and $-2.4 \lesssim$ [O/H] $\lesssim -0.4$.

After $t_{\rm age} = 0.5$ Gyr, the hot bubbles expand and blow out into the intergalactic space. As a result, more than 80 per cent of volume is occupied with highly ionized gas with $\chi_{\rm H\,I} = 10^{-6}$ to 10^{-7}. Finally, the merger of sub-galactic condensations promotes the mixing of heavy elements and weakens the spatial inhomogeneities of heavy-element abundance and ionization degree. As a result, the heavy-element abundance of ISM converges to $-0.4 \lesssim$ [Si/H] $\lesssim$ 0.1 and $-0.3 \lesssim$ [O/H] $\lesssim 0.2$ with small dispersion, and eventually 95 per cent of volume is filled with ionized gas. This means that the metallicity reaches around the solar abundance in 10^9 yr. It is consistent with the previous works on the elliptical galaxy formation (Arimoto & Yoshii 1987; Gibson 1997; Kodama & Arimoto 1997; Kawata & Gibson 2003a,b). The mean value of mass-weighted heavy-element abundance is [Si/H] $\simeq -1.0$ and [O/H] $\simeq -0.9$ at the LAE phase, while [Si/H] $\simeq -0.4$ and [O/H] $\simeq -0.3$ at the LBG phase. These are translated into the mass-weighted metallicity as $0.14\,{\rm Z}_\odot$ at LAE phase and $0.52\,{\rm Z}_\odot$ at LBG phase, which are concordant with the observations by Pettini et al. (2001) and Mannucci et al. (2009).

The luminosity of Lyman α emission, which is the cooling radiation by interstellar gas, reaches 2.0×10^{43} erg s^{-1} at $t_{\rm age} = 0.1$ Gyr and 1.6×10^{43} erg s^{-1} at $t_{\rm age} = 0.3$ Gyr, respectively. They nicely match the observed luminosity of LAEs and also well resemble LAEs with respect to other properties. After $t_{\rm age} \leq 0.5$ Gyr, the Lyman α luminosity quickly declines to several 10^{41} erg s^{-1} that is lower than the detection limit. Then, the galaxy shifts to a stellar continuum radiation-dominated phase, which appears like LBGs (see Mori & Umemura 2006).

3.2 Escape fractions

Fig. 2 shows the time evolution of escape fractions of ionizing photons derived by the full radiation transfer calculations. The upper panel represents the absolute escape fractions, which are defined by

$$f_{\rm esc} \equiv \frac{N^{\gamma}_{\rm esc}}{N^{\gamma}_{\rm total}}, \qquad (2)$$

where $N^{\gamma}_{\rm total}$ is the total number of pristine photons radiated from stars and $N^{\gamma}_{\rm esc}$ is the number of photons escaped from the simulation box. Filled circles in the upper panel of Fig. 2 represent the resultant escape fractions $f_{\rm esc}$ with dust extinction. In the LAE phase, $f_{\rm esc} =$ 0.47 at $t_{\rm age} = 0.1$ Gyr and $f_{\rm esc} = 0.23$ at $t_{\rm age} = 0.3$ Gyr, while in the LBG phase, $f_{\rm esc} = 0.19$ at $t_{\rm age} = 0.5$ Gyr and $f_{\rm esc} = 0.17$ at $t_{\rm age} = 1.0$ Gyr. The escape fractions have the dependence on the size distributions of dust, since smaller grains result in lager extinction for a given dust-to-gas ratio. If we extend the range to smaller grains as 0.02–1.0 μ m, the escape fractions are reduced to $f_{\rm esc} = 0.1-0.3$ in the LAE phase and $f_{\rm esc} = 0.09-0.1$ in the LBG phase. If the grains are even smaller as 0.03−0.3 μ m, the escape fractions become $f_{\rm esc} = 0.07 - 0.22$ in the LAE phase and $f_{\rm esc} =$ 0.06−0.07 in the LBG phase. These values are concordant with the estimations for LBGs by Shapley et al. (2006) and Iwata et al. (2009).

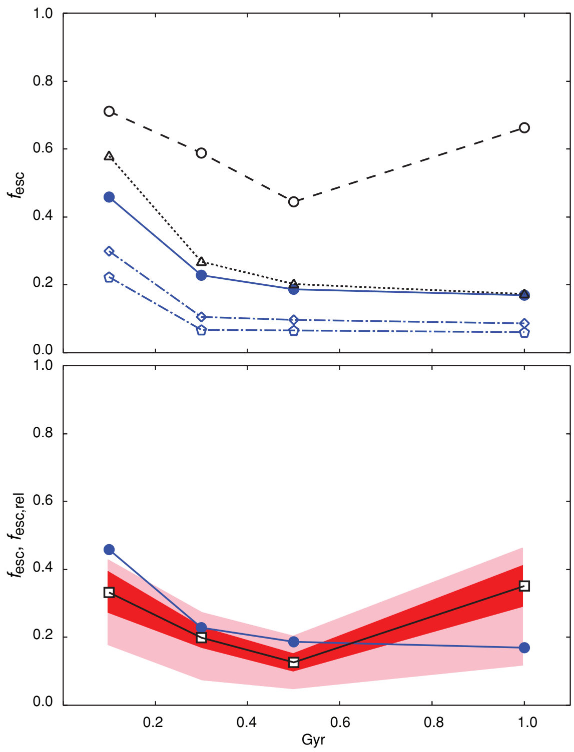

Figure 2. Upper panel: absolute escape fractions $f_{\rm esc}$ for the simulated galaxy as a function of evolutionary time. Blue symbols represent the escape fractions $f_{\rm esc}$ with dust extinction, where blue filled circles, open diamonds and open pentagons show the escape fraction for dust size of 0.1–1.0 μm, 0.02–1.0 μm and 0.03–0.3 μm, respectively. Black open circles denote $f_{\rm esc}$ without dust extinction. The black open triangles show the dust sputtering model. Lower panel: absolute escape fractions $f_{\rm esc}$ for dust size of 0.1–1.0 μm are compared to relative escape fractions $f_{\rm esc,rel}$ that are derived from the flux density ratio at 1500 to 900 Å (see equation 1). The filled circles represent the absolute escape fractions $f_{\rm esc}$ and the open squares the relative escape fractions $f_{\rm esc,rel}$. The variations by viewing angles are represented by a pink belt with the standard deviation shown by a narrower red belt.

The escape fractions are significantly regulated by interstellar dust. In Fig. 2, we also show the dust-free model (open circles), where the absorption by interstellar dust is artificially switched off. We find that the dust extinction reduces $f_{\rm esc}$ by a factor of 1.5–8.5 in the LAE phase. On the other hand, the reduction by dust extinction is a factor of 2.5−11 in the LBG phase. The change of the reduction factor is linked to the enrichment of heavy elements in the galaxy.

Gnedin et al. (2008) have shown that the escape fractions are as small as a few per cent, which is much smaller than the present results. In the calculations by Gnedin et al. (2008), most of the young stars are distributed in the dense region of galactic disc. In our model, stars are extendedly distributed, and also the bulk of interstellar gas is collisionally ionized by the SN shock heating. Since the ISM is moderately optically thin for ionizing photons, ionizing photons can escape through collisionally ionized regions. To assess the effects of collisional ionization, we have tentatively calculated a case assuming $T = 10^4$ K and no collisional ionization.

As a result, we have found that the escape fractions are reduced to $f_{\rm esc} = 0.21$ at $t_{\rm age} = 0.1$ Gyr and $f_{\rm esc} = 0.13$ at $t_{\rm age} = 1.0$ Gyr. This implies that the collisional ionization by shocks can contribute to enhance the escape fractions by a factor of 2.

If dust grains are in high-temperature regions with $T \gtrsim 10^6$ K, they may be destructed by sputtering process. The grain radius $a_{\rm d}$ decreases at a rate $da_{\rm d}/dt = -n_{\rm p}h_{\rm w}\,[1 + (T_{\rm s}/T)^{2.5}]^{-1}$ cm s^{-1} (Draine & Salpeter 1979; Tsai & Mathews 1995; Mathews & Brighenti 2003), where $h_{\rm w} = 3.2 \times 10^{-18}$ cm^4 s^{-1} and $T_{\rm s} = 2 \times 10^6$ K are fitting parameters, and $n_{\rm p}$ is the proton number density. Therefore, the destruction time-scale of $\sim$0.1 μm dust is shorter than the time-scale of galaxy evolution ($\lesssim$1 Gyr) if $n_{\rm p} \gtrsim 10^{-4}$ cm^{-3} and $T \gtrsim 10^6$ K. Since the present model galaxy has $n_{\rm p} \gtrsim 10^{-4}$ on average in high-temperature regions, we roughly suppose that all dust in high-temperature regions ($T \gtrsim 10^6$ K) is evaporated by sputtering. Open triangles in the upper panel of Fig. 2 show the escape fractions when taking the sputtering into account. After including dust sputtering, $f_{\rm esc} = 0.58$ at $t_{\rm age} = 0.1$ Gyr and $f_{\rm esc} = 0.17$ at $t_{\rm age} = 1.0$ Gyr. At higher redshifts, the dust sputtering somewhat enlarges the escape fractions, because a part of interstellar dust is distributed in high-temperature regions. On the other hand, at lower redshifts, the results are basically the same as no-sputtering cases, since ionizing photons are mainly absorbed by dust in low-temperature star-forming regions. Although the sputtering model here may overestimate the destruction of dust, the escape fractions do not change very much by including the dust sputtering. Also, in our simulations, the dust temperature does not rise over 100 K by photoheating. Since the evaporation temperature of silicate dust is $\sim$10^3 K, the photodestruction of dust is unimportant.

In order to evaluate the relative escape fractions defined by (1), we make a mock observation of the simulated galaxy using the flux density ratio at 1500 to 900 Å. Assuming $(L1500/L900)_{\rm int} = 3$ (Steidel et al. 2001) and $Q(1500\,\text{Å}) = 1$, and also that the radiation flux at 1500 Å is absorbed only by interstellar dust, we compute the transport of the radiation fluxes at 900 and 1500 Å. The resultant relative escape fractions $f_{\rm esc,rel}$ are shown by open squares in the lower panel of Fig. 2. It turns out that the predicted relative escape fractions ($f_{\rm esc,rel} \sim 0.1$–0.3) match the average of observed relative escape fractions as 0.14 (Shapley et al. 2006). Also, it is consistent with the observational estimates given by Steidel et al. (2001), Giallongo et al. (2002), Inoue et al. (2005) and Inoue, Iwata & Deharveng (2006).

4 DISCUSSION

Shapley et al. (2006) estimated $f_{\rm esc,rel}$ for 14 LBGs in the SSA22a field, and they detected ionizing photons from only two LBGs, that is C49 and D3. The reported relative escape fractions of two LBGs are extremely high as $f_{\rm esc,rel}$(C49) = 0.65 and $f_{\rm esc,rel}$(D3) $\geq$ 1.0. For the other 12 LBGs, only upper limits are suggested. Iwata et al. (2009) reported the results of Subaru/Suprime-Cam deep imaging observations of the same field. They detected ionizing radiation from seven LBGs as well as from 10 LAE candidates. They also showed the large scatter of the observed UV to Lyman continuum flux density ratios. For the seven detected LBGs, the ratio ranges from 2.4 to 23.8 with a median value of 6.6. Then, the relative escape fractions for seven LBGs range from 0.03 to 0.30 after a correction for dust extinction and can be 0.05–0.55 if IGM extinction is taken into account. In addition, some of the detected galaxies show significant spatial offsets of ionizing radiation from non-ionizing UV emission.

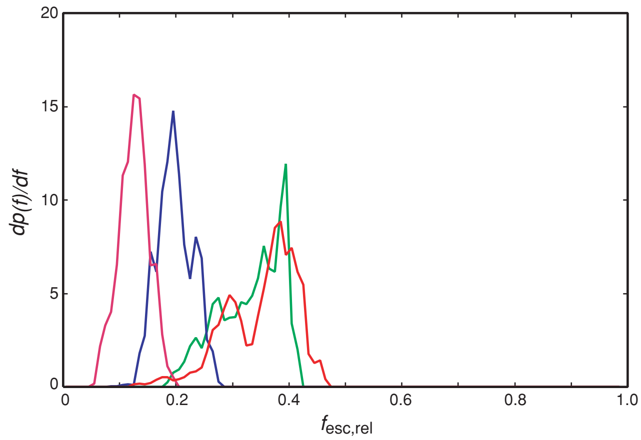

Figure 3. Probability distribution of relative escape fractions. Each line corresponds to the probability distribution at $t_{\rm age} = 0.1$ Gyr (green), 0.3 Gyr (blue), 0.3 Gyr (magenta) and 1.0 Gyr (red), respectively.

The spatial distributions of interstellar dust are highly inhomogeneous in LAEs, because it should follow the inhomogeneous heavy-element distributions (see also Mori, Ferrara & Madau 2002; Mori, Umemura & Ferrara 2004). Therefore, the observed escape fractions strongly depend on viewing angles. We compute the probability distribution function, $dp(f)/df \equiv N(f)/N_{\rm total}$, as a function of relative escape fraction along a line-of-sight, where $N_{\rm total} = 128^2$ is the total number of bins in viewing angles and $N(f)$ is the number of angular bins with a given escape fraction f. Fig. 3 shows the probability distribution function from redshift $t_{\rm age} = 0.1$ to 1.0 Gyr. This figure clearly shows that the relative escape fractions vary by viewing angles significantly. For example, depending on viewing angles, the relative escape fractions $f_{\rm esc,rel}$ vary from 0.18 to 0.43 at $t_{\rm age} = 0.1$ Gyr and from 0.12 to 0.47 at $t_{\rm age} = 1.0$ Gyr. These probability distributions are indicated by a pink belt in the lower panel of Fig. 2. The standard deviation at each redshift is also shown by a red belt. This effect allows some of the observed LAEs and LBGs to have as high an escape fraction as reported by Iwata et al. (2009).

The present analysis shows the absolute escape fractions $f_{\rm esc}$ for LAEs and LBGs can be as large as $f_{\rm esc} \gtrsim 0.17$. Hence, LAEs and LBGs are potential sources for the IGM ionization at $z \gtrsim 4$. Here, we quantify the contributions of LAEs and LBGs to the IGM ionization. Specifically, we assess the emission rate of ionizing photons from LAEs and LBGs per unit comoving volume. The emission rate is evaluated from the star formation rate based on the observed luminosity functions, with coupling the escape fractions for LAE and LBG phases obtained in the present analysis. We use the average escape fraction $\langle f_{\rm esc}\rangle = 0.35$ for the LAE phase and $\langle f_{\rm esc}\rangle = 0.18$ for the LBG phase.

In Fig. 4, the emission rate of ionizing photons per comoving Mpc^3 is shown as a function of redshift. Open symbols depict the emission rate for the samples of LAEs that are listed in the caption. Filled symbols show the emission rate for LBGs, which is estimated by extrapolating the luminosity function to $L = 0.1L^*_{z=3}$ from Steidel et al. (1999) with dust extinction of $E(B-V) = 0.13$ (see also Yoshida et al. 2006). As a theoretical criterion, we adopt that by Madau, Haardt & Rees (1999), where the emission rate of ionizing photons required to balance the recombination is given by $\dot{N}_{\rm ion} = 10^{47.4}C(1+z)^3{\rm s}^{-1}{\rm Mpc}^{-3}$. C is the clumping factor which parametrizes the inhomogeneity of ionized hydrogen in the IGM. Madau et al. (1999) adopted $C = 30$, based on the value computed by

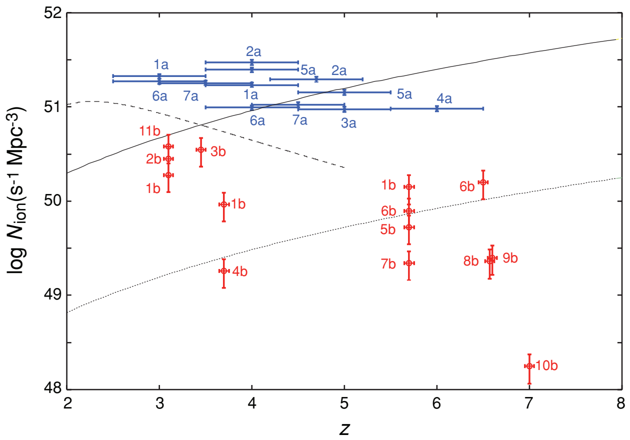

Figure 4. The evolution of emission rate of ionizing photons per comoving Mpc, $\dot{N}_{\rm ion}$, as a function of redshift. The blue filled symbols represent the $\dot{N}_{\rm ion}$ of LBGs derived from (1a) Steidel et al. (1999), (2a) Yoshida et al. (2006), (3a) Iwata et al. (2003), (4a) Bouwens et al. (2006), (5a) Ouchi et al. (2004), (6a) Sawicki & Thompson (2006) and (7a) Gabasch et al. (2004) with $\langle f_{\rm esc}\rangle = 0.18$ which is the mean escape fraction at LBG phase. Open red symbols represent $\dot{N}_{\rm ion}$ of LAEs derived from (1b) Ouchi et al. (2008), (2b) Kudritzki et al. (2000), (3b) van Breukelen, Jarvis & Venemans (2005), (4b) Fujita et al. (2003), (5b) Ajiki et al. (2003), (6b) Malhotra & Rhoads (2004), (7b) Rhoads et al. (2003), (8b) Kodaira et al. (2003), (9b) Taniguchi et al. (2005), (10b) Iye et al. (2006) and (11b) Gronwall et al. (2007) with $\langle f_{\rm esc}\rangle = 0.35$ which is mean escape fraction at LAE phase. The horizontal and vertical error bars arise from the uncertainty of observations and the variation of escape fractions (LAE: $f_{\rm esc} = 0.22$–0.47, LBG: $f_{\rm esc} = 0.17$–0.19), respectively. The solid and dotted lines indicate the emission rate required to ionize the IGM with $C = 30$ and $C = 1$, respectively (Madau et al. 1999). The dashed line represents the emission rate evaluated by the QSO luminosity function shown in Madau et al. (1999).

a cosmological radiative transfer simulation of Gnedin & Ostriker (1997). Ouchi et al. (2004) also adopted $C = 30$ when computing the number of ionizing photons needed to keep the IGM highly ionized at $z = 5$, as do a number of other authors. Although C may have some uncertainty, we assume $C = 30$ here as a fiducial value.

Fig. 4 clearly illustrates that observed LBGs can provide the majority of ionizing photons at $z = 3-5$ and play an important role to keep the Universe ionized. However, LAEs are not capable of ionizing large volumes at the redshift $z = 3-5$. On the other hand, ionizing photons from not only LBGs but also LAEs are not enough to ionize the IGM at $z \gtrsim 6$. Most of photons that ionize the Universe may come from undetected faint LAEs and LBGs or other sources. Recently, Choudhury & Ferrara (2007) studied the cosmic reionization history to account for a number of observational data and pointed out that low-mass galaxies hosting Pop III stars can be predominant ionizing sources of the IGM at high z. Our results advocate their model. In the present analysis, all Lyman α photons are assumed to escape. Hence, the contribution of LAEs may be underestimated. In the future work, we intend to include Lyman α line transfer to compare the numerical results more precisely with the observations.

5 SUMMARY

We have performed 3D radiation transfer calculations, based on a high-resolution hydrodynamic simulation of an SN-dominated primordial galaxy, to obtain the ionization structure and explore the escape fractions of ionizing photons from LAEs and LBGs at high redshifts. The effect of dust extinction is incorporated according to the chemical enrichment, taking the size distributions of dust into account. As a result, we find that dust extinction reduces the escape fractions by a factor of 1.5–8.5 in the LAE phase and by a factor of 2.5–11 in the LBG phase. The resultant escape fractions are 0.07–0.47 in the LAE phase and 0.06–0.17 in the LBG phase. These results are well concordant with recent observations. We have found that the combination of diffuse distributions of stars and SN shock heating is important for UV escape fractions. In the present galaxy model, young stars are extendedly distributed, and also the bulk of interstellar gas is collisionally ionized by SN shock heating. Since the ISM is moderately optically thin and quite bubbly, ionizing photons can escape through collisionally ionized regions. The collisional ionization by shocks contributes a factor of ≈2 to the increase of the escape fractions.

The relative escape fractions derived by mock observations of the simulated galaxy match quite well the estimates by recent observations for LAEs and LBGs. To assess the contribution of LAEs and LBGs to the IGM ionization, the resultant escape fractions have been combined with the luminosity functions of LAEs and LBGs. As a result, we find that high-z LAEs and LBGs can ionize the IGM at $z = 3$–5. However, ionizing radiation from LAEs as well as LBGs is not enough to ionize the IGM at $z > 6$. That implies that undetected faint LAEs and LBGs or additional ionization sources may determine the IGM ionization at $z > 6$.

Very recently, Wise & Cen (2009) performed 3D radiation hydrodynamic simulations to assess the contribution of dwarf galaxies to cosmic reionization at redshift $z = 8$. They studied the UV escape fractions for low-mass galaxies in the mass range of $M_{\rm total} = 3 \times 10^6$ to 3×10^9 M$_\odot$. As a result, they have shown that the UV escape fractions can reach up to ∼0.8 without dust extinction in haloes with $>10^8$ M$_\odot$ for a top-heavy IMF. However, in order to assess the contribution of LAEs and LBGs to IGM reionization, we should evaluate the UV escape fractions from more massive galaxies with dust extinction. Here, we have shown that a high-mass, metal-enriched galaxy at low redshifts can allow escape fractions as large as some tens of per cent. We have found that an order-of-magnitude increase in the escape fractions can be attributed to the diffuse distribution of stars, while the collisional ionization further raises them by some factor.

ACKNOWLEDGMENTS

We are grateful to A. Inoue, A. Ferrara and A. Razoumov for valuable discussion and comments. Numerical simulations have been performed with the *FIRST* simulator and *T2K-Tsukuba* at the Center for Computational Sciences, University of Tsukuba. This work was supported in part by the *FIRST* project based on Grants-in-Aid for Specially Promoted Research by MEXT (16002003) and JSPS Grant-in-Aid for Scientific Research (S) (20224002), (A) (21244013) and (C) (18540242).

REFERENCES

Ajiki M. et al., 2003, AJ, 126, 2091
Alvarez M. A., Bromm V., Shapiro P. R., 2006, ApJ, 639, 621
Arimoto N., Yoshii Y., 1987, A&A, 173, 23
Bouwens R. J., Illingworth G. D., Blakeslee J. P., Franx M., 2006, ApJ, 653, 53
Bouwens R. J., Illingworth G. D., Franx M., Ford H., 2007, ApJ, 670, 928
Choudhury T. R., Ferrara A., 2007, MNRAS, 380, L6

Ciardi B., Bianchi S., Ferrara A., 2002, MNRAS, 331, 463
Draine B. T., Lee H. M., 1984, ApJ, 285, 89
Draine B. T., Salpeter E. E., 1979, ApJ, 231, 77
Dunkley J. et al., 2009, ApJS, 180, 306
Fan X. et al., 2001, AJ, 122, 2833
Fan X. et al., 2006, AJ, 132, 117
Fioc M., Rocca-Volmerange B., 1997, A&A, 326, 950
Fujita S. S. et al., 2003, AJ, 125, 13
Gabasch A. et al., 2004, A&A, 421, 41
Giallongo E., Cristiani S., D'Odorico S., Fontana A., 2002, ApJ, 568, L9
Gibson B. K., 1997, MNRAS, 290, 471
Gnedin N. Y., 2008, ApJ, 673, L1
Gnedin N. Y., Ostriker J. P., 1997, ApJ, 486, 581
Gnedin N. Y., Kravtsov A. V., Chen H.-W., 2008, ApJ, 672, 765
Gronwall C. et al., 2007, ApJ, 667, 79
Haardt F., Madau P., 1996, ApJ, 461, L20
Iliev I. T. et al., 2006, MNRAS, 371, 1057
Inoue A. K., Iwata I., Deharveng J.-M., Buat V., Burgarella D., 2005, A&A, 435, 471
Inoue A. K., Iwata I., Deharveng J.-M., 2006, MNRAS, 371, L1
Iwata I., Ohta K., Tamura N., Ando M., Wada S., Watanabe C., Akiyama M., Aoki K., 2003, PASJ, 55, 415
Iwata I. et al., 2009, ApJ, 692, 1287
Iye M. et al., 2006, Nat, 443, 186
Kawata D., Gibson B. K., 2003a, MNRAS, 340, 908
Kawata D., Gibson B. K., 2003b, MNRAS, 346, 135
Kitayama T., Yoshida N., Susa H., Umemura M., 2004, ApJ, 613, 631
Kodama T., Arimoto N., 1997, A&A, 320, 41
Kodaira K. et al., 2003, PASJ, 55, L17
Kudritzki R.-P. et al., 2000, ApJ, 536, 19
Madau P., Haardt F., Rees M. J., 1999, ApJ, 514, 648
Malhotra S., Rhoads J. E., 2004, ApJ, 617, L5
Mannucci F. et al., MNRAS, in press (arXiv:0902.2398)
Mathews W. G., Brighenti F., 2003, ApJ, 590, L5
Mathis J. S., Rumpl W., Nordsieck K. H., 1977, ApJ, 217, 425
Mori M., Umemura M., 2006, Nat, 440, 644
Mori M., Ferrara A., Madau P., 2002, ApJ, 571, 40
Mori M., Umemura M., Ferrara A., 2004, ApJ, 613, L97
Nakamoto T., Umemura M., Susa H., 2001, MNRAS, 321, 593
Osterbrock D. E., 1989, Astrophysics of Gaseous Nebulae and Active Galactic Nuclei. University Science Books, Mill Valley, CA
Ouchi M. et al., 2004, ApJ, 611, 660
Ouchi M. et al., 2008, ApJS, 176, 301
Page L. et al., 2007, ApJS, 170, 335
Pettini M., Shapley A., Steidel C. C., Cuby J.-G., Dickinson M., Moorwood A. F. M., Adelberger K. L., Giavalisco M., 2001, ApJ, 554, 981
Razoumov A. O., Sommer-Larsen J., 2006, ApJ, 651, L89
Razoumov A. O., Sommer-Larsen J., 2007, ApJ, 668, 674
Rhoads J. E. et al., 2003, AJ, 125, 1006
Salpeter E. E., 1955, ApJ, 121, 161
Sawicki M., Thompson D., 2006, ApJ, 642, 653
Shapley A. E., Steidel C. C., Pettini M., Adelberger K. L., Erb D. K., 2006, ApJ, 651, 688
Steidel C. C., Adelberger K. L., Giavalisco M., Dickinson M., Pettini M., 1999, ApJ, 519, 1
Steidel C. C., Pettini M., Adelberger K. L., 2001, ApJ, 546, 665
Susa H., Umemura M., 2000, ApJ, 537, 578
Susa H., Umemura M., 2004, ApJ, 600, 1
Taniguchi Y. et al., 2005, PASJ, 57, 165
Thoul A. A., Weinberg D. H., 1996, ApJ, 465, 608
Tsai J. C., Mathews W. G., 1995, ApJ, 448, 84
Umemura M., Ikeuchi S., 1984, Prog. Theor. Phys., 72, 47
Umemura M., Nakamoto T., Susa H., 2001, in Umemura M., Susa H., eds, ASP Conf. Ser. Vol. 222, The Physics of Galaxy Formation. Astron. Soc. Pac., San Francisco, p. 109
van Breukelen C., Jarvis M. J., Venemans B. P., 2005, MNRAS, 359, 895
Whalen D., Abel T., Norman M. L., 2004, ApJ, 610, 14
Wise J. H., Cen R., 2009, ApJ, 693, 984
Yoshida M. et al., 2006, ApJ, 653, 988

This paper has been typeset from a TEX/LATEX file prepared by the author.